

ARTICLE

Coastal and Marine Ecology

Correcting for measurement errors in a long-term aerial survey with auxiliary photographic data

Jamie L. Brusa¹  | Matthew T. Farr²  | Joseph Evenson³ |
Emily Silverman⁴ | Bryan Murphie⁵ | Thomas A. Cyra⁵ |
Heather J. Tschaekofske⁶ | Kyle A. Spragens⁶ | Sarah J. Converse⁷

¹School of Environmental and Forest Sciences, University of Washington, Seattle, Washington, USA

²Washington Cooperative Fish and Wildlife Research Unit, School of Aquatic and Fishery Sciences, University of Washington, Seattle, Washington, USA

³Washington Department of Fish and Wildlife, Bellingham, Washington, USA

⁴U.S. Fish and Wildlife Service, Division of Migratory Bird Management, Laurel, Maryland, USA

⁵Washington Department of Fish and Wildlife, Port Townsend, Washington, USA

⁶Washington Department of Fish and Wildlife, Olympia, Washington, USA

⁷U.S. Geological Survey, Washington Cooperative Fish and Wildlife Research Unit, School of Aquatic Fishery Sciences & School of Environmental and Forest Sciences, University of Washington, Seattle, Washington, USA

Correspondence

Jamie L. Brusa

Email: jamie.brusa@noaa.gov

Present address

Jamie L. Brusa, Integrated Statistics in Support of Northeast Fisheries Science Center, National Marine Fisheries Service, NOAA, Woods Hole, Massachusetts, USA.

Funding information

US Fish and Wildlife Service; Sea Duck Joint Venture; Washington Department of Fish and Wildlife; Washington Cooperative Fish and Wildlife Research Unit

Handling Editor: Hunter S. Lenihan

Abstract

Long-term, large-scale monitoring of wildlife populations is an integral part of conservation research and management. However, some traditional monitoring protocols lack the information needed to account for sources of measurement error in data analyses. Ignoring measurement error, such as partial availability, imperfect detection, and species misidentification, can lead to mischaracterizations of population states and processes. Accounting for measurement error is key to robust monitoring of populations, which can inform a wide variety of decisions, including harvest, habitat restoration, and determination of the legal status of species. We undertook an effort to retroactively minimize bias in a large-scale, long-term monitoring program for marine birds in the Salish Sea, Washington, USA, by conducting an auxiliary study to jointly estimate components of measurement error. We built a novel model in a Bayesian framework that simultaneously harnessed human observer and photographic data types to produce estimates necessary to correct for the effects of partial availability, imperfect detection, and species misidentification. Across all 31 species identified in photographs, both observers had instances of undercounting and overcounting birds but tended to undercount (observers undercounted totals across all species on 69.3%–78.9% of transects). We estimated species-specific correction factors that can be used to correct both historical and

This is an open access article under the terms of the [Creative Commons Attribution](https://creativecommons.org/licenses/by/4.0/) License, which permits use, distribution and reproduction in any medium, provided the original work is properly cited.

© 2024 The Author(s). *Ecosphere* published by Wiley Periodicals LLC on behalf of The Ecological Society of America.

future counts from the Salish Sea survey, which has been running since 1992. Our novel modeling framework can be applied in other multispecies monitoring contexts where minimal photographic data can be collected for the purposes of correcting for measurement error in large-scale, long-term datasets.

KEYWORDS

aerial survey analysis, Bayesian statistics, imperfect detection, marine birds, multispecies monitoring, species misidentification

INTRODUCTION

Robust estimates of population parameters obtained from monitoring data are valuable for wildlife research and management. However, robust estimates depend on monitoring protocols and analytical approaches designed to account for measurement errors. Raw count data from population surveys frequently result in biased measures of abundance as a result of such errors (Caughley, 1974; Davis et al., 2022; Pollock & Kendall, 1987; Russell et al., 1996; Samuel & Pollock, 1981). Ignoring measurement error may lead to either over- or underestimation of parameters, such as population abundance. Measurement error can arise from multiple sources, including partial availability, imperfect detection, or species misidentification. Partial availability occurs when animals flee from observers before they are detected or exhibit other cryptic behaviors (e.g., diving under water). Imperfect detection occurs when observers fail to detect animals that are available. Finally, even when individuals of a species are counted accurately, they may be misidentified as members of another species (Miller et al., 2011). Often, these processes occur simultaneously during data collection and may not be readily apparent to observers. A variety of survey methods and corresponding statistical models, such as detection/non-detection data and occupancy modeling (MacKenzie et al., 2002; Miller et al., 2011) or repeated count data and N-mixture models (Royle & Nichols, 2003), may be adopted to account for such measurement errors.

Monitoring across large geographic areas is often conducted through aerial surveys (Briggs et al., 1985a; Buckley & Buckley, 2000; Chabot et al., 2018; Siniff & Skoog, 1964). Established methods for estimating observation error in aerial surveys include distance sampling (Buckland et al., 2001), double-observer methods (Cook & Jacobson, 1979), simultaneous observations from multiple platforms, such as plane and ship (Briggs et al., 1985b), or estimation of correction factors using comparisons of observed aerial counts to a known number of decoys (Frederick et al., 2003; Strobel & Butler, 2014). However, each of these methods has potential drawbacks, including additional assumptions or higher

resource (e.g., time, money) demands. Distance sampling is a useful method but can be challenging to implement in aerial surveys because observers must record exact distances or distance bins in addition to counting and identifying species, which is often not feasible for large groups composed of multiple species (e.g., Davis et al., 2022); further, distance sampling cannot directly accommodate partial availability. Double observer methods and counts from multiple platforms are typically more expensive, do not address partial availability and can, for some species, be difficult to implement in practice (Briggs et al., 1985b; Pollock & Kendall, 1987; Samuel & Pollock, 1981). Using decoys to develop correction factors can have limited applicability if decoys do not reasonably mimic the behaviors of live animals.

Photographs taken from aerial platforms are a promising approach, especially as autonomous aerial vehicles become more readily available and affordable. As photographs allow for identifying and counting species without a time limit, these methods may eliminate or substantially reduce measurement error associated with imperfect detection and species misidentification. However, long-term collection and analysis of aerial photographs currently tends to be more costly and time-intensive than observer-led surveys and can be logistically prohibitive for large landscapes (Bayliss & Yeomans, 1990; Béchet et al., 2004; Watson, 1969). Using autonomous aerial systems not only tends to lower costs and risks to observer safety, but it can also introduce challenges that existing technology has not yet overcome, such as additional sound disturbance, privacy issues, limitations on the duration of flights (Wang et al., 2019), time-consuming processing procedures, and high sensitivity to inclement weather (e.g., Weiser et al., 2022). Additionally, photographs with poor contrast between animals and their background, or including heavy cover that conceals animals, can create difficulties in identifying species or detecting individual animals, which can lead to large biases in abundance estimates (Brack et al., 2018; Siniff & Skoog, 1964). Finally, photographs provide only a single snapshot whereas human observers usually have several seconds to observe animals, which may improve species

identification. However, whereas photography alone may have weaknesses as a monitoring method, coupling photographs with observer counts in aerial surveys can support estimation of reliable correction factors for observer counts and can serve as a cost-effective approach to improve observer-led wildlife monitoring (Bayliss & Yeomans, 1990; Lamprey et al., 2020).

Numerous marine bird species are either residents of or overwinter in the Salish Sea, an ecologically, economically, and culturally important ecosystem in the North American portion of the Pacific flyway (Crewe et al., 2012; Gaydos & Pearson, 2011). The Washington Department of Fish and Wildlife has monitored wintering marine birds in the US portion of the Salish Sea annually since 1992 using strip-transect aerial surveys. These surveys have provided consistent evidence for declining abundances of multiple marine bird species (Anderson et al., 2009; Bower, 2009; Vilchis et al., 2014). Accurate abundance estimates are valuable for guiding decision-making processes, for example, regarding harvest, habitat restoration, and legal protection for declining species. Additionally, marine birds have been identified as important indicators of ecosystem health in the Salish Sea (Bishop et al., 2016; Blight et al., 2015; Miller et al., 2015; Pearson & Hamel, 2013), increasing the importance placed on monitoring these species. Aerial surveys are a particularly important method for monitoring marine birds in this region because some sections of the Salish Sea are difficult to access by other means (Vilchis et al., 2014).

Here, we present a novel model designed to correct for measurement error in aerial survey counts of marine birds. Our model integrates observer and photographic data collected simultaneously during a one-time aerial survey and is designed to account for several sources of measurement error, including partial availability, imperfect detection, and species misidentification. We applied the model to develop correction factors that can be used to correct counts from both past and future aerial surveys. Our model can be applied to any monitoring situation in which limited photographic data can be collected, simultaneously with observer counts, for the purpose of calculating correction factors that can then be used to correct a larger dataset of observer counts.

METHODS

Data collection

Data collection from a high-wing de Havilland DHC-2 aircraft on floats occurred over 5 days in March 2012 in a portion of the Salish Sea, Washington, USA (48° N, 123° W), known to contain a high diversity of

overwintering marine bird species. Surveys were designed using a strip transect method with a strip width of 50 m on the left side of the plane. A 0.64-cm poly line tied to the wing strut at 33° and the edge of the floats at 58° created visual boundaries for the transect. The aircraft flew at a speed of 157–167 km/h at an altitude of about 61 m; the plane flew directly into the wind to maintain a forward orientation. Each transect was about 2 km long and took, on average, 44 s to complete. A total of 625 transects were flown over the 5-day study, capturing 175,680 photographs.

Two experienced observers (17 and 15 years of experience for observers 1 and 2, respectively) sat in the middle and rear seats on the left side of the aircraft, and the aircraft landed once per day for observers to switch seats. Observers recorded the number of birds detected and identified each bird to the lowest taxonomic group possible (usually species). Observers did not communicate with each other during data collection and were visually separated by an opaque divider. The observer in the middle seat had a slightly larger window than the observer in the rear seat; only the middle seat is used during standard surveys. Observers recorded an index of glare and the Beaufort sea-state during surveys. However, we did not include either of these variables in our analyses because glare had negligible variation across transects, and Beaufort sea-state varied within transects, which were our unit of analysis.

Meanwhile, a Canon EOS 5D Mark II equipped with a Canon EF 70-200 mm f/2.8 L IS USM lens set to 200 mm, attached high on the wing strut to eliminate vibrations from the propeller, captured photographs of birds. This forward-facing camera took continuous photographs at 3.9 frames per second imaging the transect strip from 250–270 m ahead of the aircraft to 500–540 m ahead, often capturing the same birds in multiple images. An additional camera, the point-of-view camera, was mounted to photograph the transect at the same time as the observers viewed the same section of transect. To delineate the 50-m-wide transect strip, both the forward-facing and point-of-view cameras were calibrated to the transect strip at the start of each survey day by flying at various altitudes above and parallel to straight highway and railway lines positioned in the same direction as the wind. The aircraft flew two passes into the wind and parallel to the road or railway and took photographs with both cameras when the aircraft was flying level (with vertical, lateral, and longitudinal axes of 0°), and when the road or railway matched the outer edge of the aircraft float (58°) or a marking on the wing strut delineating the outer boundary of the transect strip (34.5°). The positions of the inner and outer boundaries based on the imaged road or railway lines were then transposed on each photograph taken during that survey

day. The point-of-view camera was designed to capture the area simultaneously seen by observers and the same section of transect the forward-facing camera captured (aircraft speed could be used to pair forward-facing and point-of-view camera images; the point-of-view camera captured the same section of transect 6–8 s following the forward-facing camera depending on the speed of the plane). However, the field of view from the point-of-view camera proved to be different from that of observers (the camera was aimed abeam of the aircraft, i.e., perpendicular to the flight direction of the aircraft, while the observers could see abeam as well as behind and ahead), limiting its usefulness. Therefore, we did not use the point-of-view camera in the analysis. We do not refer to the point-of-view camera further; hereafter, “camera” refers to the forward-facing camera only. The in-flight observers synchronized their watches with the clocks on the cameras and GPS to allow for accurate image matching to the observer records.

An independent observer, not present on any of the flights, counted and identified to the lowest taxonomic group possible (usually species) each bird in each photograph from the camera. This observer could identify species from multiple angles using multiple photographs. We used data from 321 of the 625 completed transects for analyses. As the focus of the study was to derive correction factors for sea ducks (Tribe Mergini), transects were randomly selected from a group where the observers recorded sea ducks or where the transects were over habitats used by sea ducks. In addition, randomly selected transects from this group were prioritized such that all Beaufort sea states and glare categories were represented. See Evenson et al. (2013) for full details on data collection, including camera placement and photo processing.

Analytical approach

We assume that the bird species composition and abundance data captured by the camera represent the population of interest. Some small differences between the true composition and abundance and what was observed in the photographs may occur because foraging marine birds dive (independent of a response to the plane) and, thus, are not always available, and because 100% of all birds in the photographs could not be identified to species. By contrast, the observer data potentially contained multiple sources of measurement error. We identified three sources of measurement error: (1) movement of birds in response to the plane, (2) misidentification of species, and (3) imperfect detection of birds. Movement in response to the plane may not only include

diving or flying out of the transect but may also include flying into the transect or surfacing after the camera passed over their location. Species misidentification occurs if an observer detects an individual but incorrectly identifies it. Imperfect detection of birds occurs if an observer misses an entire group of one or more individuals, or if they under- or overcount the number of individuals in a detected group. Many marine birds form large and mixed-species groups during the winter, and some species have quite similar physical characteristics, for example, Common Goldeneye (*Bucephala clangula*) and Barrow’s Goldeneye (*Bucephala islandica*), which may contribute to imperfect detection or misidentification.

Birds in photographs could not always be identified to species (~7% of marine birds, excluding gulls and scaup, could not be identified to species). Because the photographic data were used as truth in the analysis, this limited our ability to fully account for species misidentification. To develop species-specific abundances despite this limitation, we allocated the individuals in species groups identified in photographs to appropriate species in proportion to their occurrence in the photographic detections that were identified to species across the entire dataset (Table 1; Conn et al., 2012). For example, if 450 Common Goldeneye, 50 Barrow’s Goldeneye, and 200 unclassified goldeneyes were recorded in photographs, $450/(50 + 450) = 90\%$ (180) of the unclassified goldeneyes would be allocated to the count of Common Goldeneye and the remainder to Barrow’s Goldeneye. In this way, we eliminated groups recorded as “unclassified goldeneye” in the dataset. For the observer data, we left counts in species groups unchanged. The model then dealt with these as misidentifications using the methods described below. The assumption implicit in our approach—that the relative abundance of unidentifiable individuals within species groups is proportional to the relative abundance of identifiable individuals within species groups in photographs—may not be perfectly met, and, therefore, we ran two analyses: a taxonomically fine-filtered analysis and a taxonomically coarse-filtered analysis. In the taxonomically coarse-filtered analysis, we defined species groups to a higher taxonomic level (e.g., “goldeneye”) rather than assigning them to species as described above. Additionally, given challenges with identification and the goals of the monitoring program, gulls (likely *Larus* spp. and *Chroicocephalus* spp. in the Salish Sea in winter) were not identified beyond species group even in the fine-filtered analysis. We also treated scaup, including Greater Scaup (*Aythya marila*) and Lesser Scaup (*Aythya affinis*), as a single group given the challenges in distinguishing them.

TABLE 1 Species and species groupings of marine birds identified from photographs taken during aerial surveys in the Salish Sea, Washington, USA.

Species (i.e., fine-grained)	Species group (i.e., coarse-grained)	Scientific name	Counts
Ancient Murrelet	Alcid ^a	<i>Synthliboramphus antiquus</i>	0, 6, 1
Common Murre	Alcid	<i>Uria aalge</i>	29, 40, 63
Marbled Murrelet	Alcid	<i>Brachyramphus marmoratus</i>	51, 9, 104
Pigeon Guillemot	Alcid	<i>Cephus columba</i>	24, 34, 88
Rhinoceros Auklet	Alcid	<i>Cerorhinca monocerata</i>	103, 89, 377
Unclassified alcid ^b	Alcid	NA	6, 4, 4
Unclassified small alcid ^b	Alcid	NA	0, 1, 2
Unclassified murrelet ^b	Alcid	NA	0, 8, 26
Brant	Brant	<i>Branta bernicla</i>	1566, 1195, 1190
Bufflehead	Bufflehead	<i>Bucephala albeola</i>	1196, 991, 1659
Double-crested Cormorant	Cormorant	<i>Phalacrocorax auritus</i>	6, 15, 22
Pelagic Cormorant	Cormorant	<i>Phalacrocorax pelagicus</i>	7, 9, 66
Unclassified cormorant ^b	Cormorant	NA	50, 36, 65
American Wigeon	Dabbling duck ^c	<i>Mareca americana</i>	496, 258, 1055
Eurasian Wigeon	Dabbling duck	<i>Mareca penelope</i>	0, 0, 10
Mallard	Dabbling duck	<i>Anas platyrhynchos</i>	22, 10, 66
Northern Pintail	Dabbling duck	<i>Anas acuta</i>	90, 2, 138
Barrow's Goldeneye	Goldeneye	<i>Bucephala islandica</i>	29, 19, 30
Common Goldeneye	Goldeneye	<i>Bucephala clangula</i>	90, 32, 174
Unclassified goldeneye ^b	Goldeneye	NA	68, 44, 61
Horned Grebe	Grebe	<i>Podiceps auritus</i>	55, 41, 221
Red-necked Grebe	Grebe	<i>Podiceps grisegena</i>	46, 7, 52
Western Grebe	Grebe	<i>Aechmophorus occidentalis</i>	254, 194, 399
Unclassified grebe ^b	Grebe	NA	0, 4, 9
Gull ^d	Gull	NA	515, 422, 726
Harlequin Duck	Harlequin Duck	<i>Histrionicus histrionicus</i>	36, 21, 74
Long-tailed Duck	Long-tailed Duck	<i>Clangula hyemalis</i>	320, 260, 402
Common Loon	Loon	<i>Gavia immer</i>	59, 25, 89
Pacific Loon	Loon	<i>Gavia pacifica</i>	3, 8, 18
Red-throated Loon	Loon	<i>Gavia stellata</i>	51, 84, 98
Unclassified loon ^b	Loon	NA	41, 22, 121
Common Merganser	Merganser	<i>Mergus merganser</i>	1, 2, 1
Red-breasted Merganser	Merganser	<i>Mergus serrator</i>	57, 19, 104
Unclassified merganser ^b	Merganser	NA	4, 62, 20
Ruddy Duck	Ruddy Duck	<i>Oxyura jamaicensis</i>	26, 5, 30
Scaup ^e	Scaup	NA	90, 75, 124
Black Scoter	Scoter	<i>Melanitta americana</i>	0, 0, 2
Surf Scoter	Scoter	<i>Melanitta perspicillata</i>	691, 560, 993
White-winged Scoter	Scoter	<i>Melanitta deglandi</i>	129, 92, 450
Unclassified scoter ^b	Scoter	NA	158, 171, 107

(Continues)

TABLE 1 (Continued)

Species (i.e., fine-grained)	Species group (i.e., coarse-grained)	Scientific name	Counts
Unclassified duck ^b	f	NA	0, 75, 79
Unclassified seabird ^b	f	NA	11, 0, 79

Note: To account for unclassified birds even in the reference (i.e., camera) data, we conducted two analyses, a taxonomically fine-grained analysis and a coarse-grained analysis. The classes in the fine-grained and coarse-grained analyses are shown, along with scientific names for species. Counts are presented as observer 1, observer 2, camera, with camera counts in boldface.

^aAlcids are members of the family Alcidae.

^bIn the taxonomically fine-grained analysis, counts of the following groups were allocated proportional to the counts for individuals within the group that were identified to species, as follows: “unclassified alcid” to all alcids; “unclassified small alcid” to all murrelets; “unclassified murrelet” to all murrelets; “unclassified cormorant” to all cormorants; “unclassified goldeneye” to all goldeneyes; “unclassified grebe” to all grebes; “unclassified loon” to all loons; and “unclassified merganser” to all mergansers. The species group “unclassified duck” was allocated proportionally across all ducks (i.e., Bufflehead, all dabbling ducks, all goldeneyes, Harlequin Duck, Ling-tailed Duck, all mergansers, Ruddy Duck, scaup, and all scoters). The species group “unclassified seabird” was allocated proportionally across all other species.

^cDabbling ducks are members of the family Anatidae, subfamily Anatinae.

^dGiven challenges with identification and the objectives of the monitoring program, we grouped all gulls (family Laridae), likely including *Larus* spp. and *Chroicocephalus philadelphia*, in both the fine-grained and coarse-grained analyses.

^eScaup are composed of two species, Greater Scaup (*Aythya marila*) and Lesser Scaup (*Aythya affinis*), but because of challenges in distinguishing them, they were never identified to species in the survey data.

^fIn the taxonomically coarse-grained analysis, counts of the following groups were allocated proportionally to species groups as follows: “unclassified duck” to Bufflehead, dabbling ducks, goldeneyes, Harlequin Duck, Long-tailed Duck, mergansers, Ruddy Duck, scaup, and scoters; “unclassified seabird” to all species groups.

Camera

We summarized observations from the camera including birds flying and birds on the surface of the water, giving us a count, FF_{ji} , for transect j and species i . We assumed the camera contained no measurement error and captured the true abundance of birds available within the field of view. To estimate species composition in each transect, j , we described FF_{ji} , using a multinomial distribution as shown in Equation (1) (Figure 1):

$$FF_{ji} \sim \text{multinomial}\left(\pi_i, \sum_i FF_{ji}\right), \quad (1)$$

where π_i is the bird species composition pre-aircraft contact (i.e., the proportion of birds on the transect that are members of each species i), and $\sum_i FF_{ji}$ is the total bird abundance (i.e., the summation of the data across species, i , within each transect, j). We described the species-wide bird abundance on transect j in Equation (2) using a Poisson distribution with mean species-wide bird abundance, Λ :

$$\sum_i FF_{ji} \sim \text{Poisson}(\Lambda). \quad (2)$$

We used the forward-facing camera data to estimate π_i and Λ . We parameterized species composition as: $\pi_i = \lambda_i / \Lambda$, where λ_i is the expected species-specific mean abundance. We constrained $\Lambda = \sum_i \lambda_i$, which implies Equation (3):

$$FF_{ji} \sim \text{Poisson}(\lambda_i). \quad (3)$$

The following subsections describe a method to estimate the three parameters associated with each type of measurement error (i.e., movement, species misidentification, and imperfect detection). However, we found that disentangling these three parameters can prove difficult in practice. Therefore, we follow the presentation of that analytical method with a condensed method that estimates those three parameters as one parameter to capture the total measurement error generated from movement, imperfect detection, and species misidentification.

Movement

The observer’s field of view is on the side of the aircraft; thus, observers count birds after they come into contact with the aircraft (i.e., are nearly or directly below the aircraft). Individual birds may move into or out of view at random or due to a behavioral response to the aircraft. The available latent abundance for observers is, therefore, an outcome of species-wide abundance and a movement process. We used Equation (4) to describe available latent species-wide abundance, $\Sigma_i N_{ji}$, as the summation of individuals captured by the camera for each species i and transect j after aircraft contact:

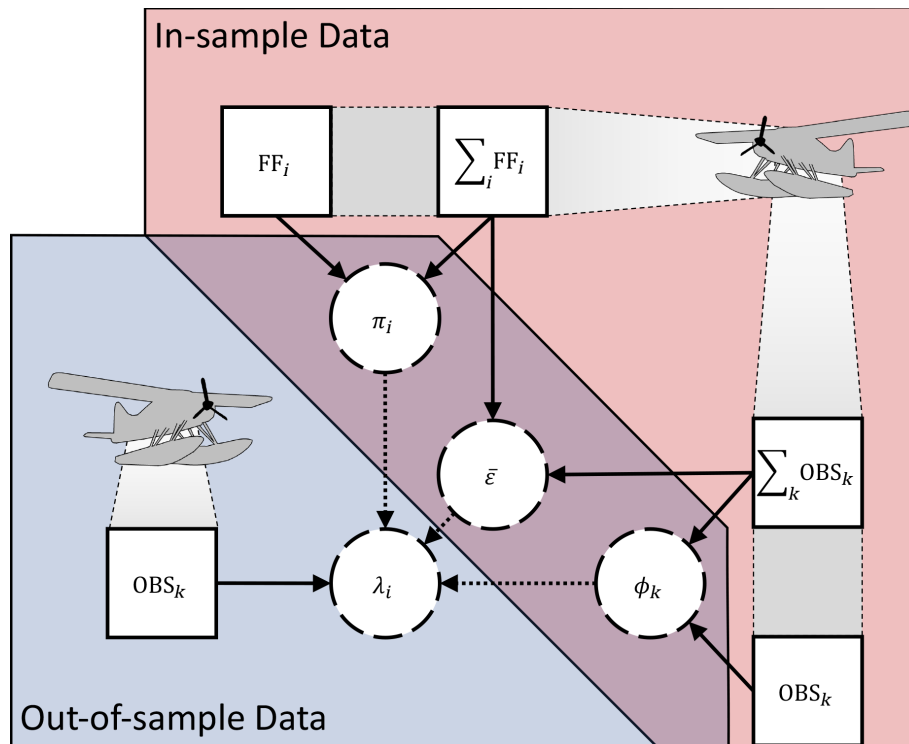


FIGURE 1 Directed acyclic graph showing relationship between in-sample data and out-of-sample correction. Boxes are data, and dashed circles are parameter values. Solid arrows represent relationships between data and parameters. Dashed arrows indicate information used to correct the out-of-sample data.

$$\sum_i N_{ji} \sim \text{Poisson}(\Lambda \times \bar{\alpha}), \tag{4}$$

where $\bar{\alpha}$ is the mean of the species-specific movement, α_i , which captures movement rates of individual species. The support for the movement rate is 0 to ∞ , which allows for individuals to move both in and out of the observers' field of view, where $\bar{\alpha} < 1$ indicates more birds moving out of the field of view than in, $\bar{\alpha} > 1$ indicates more birds moving into the field of view than out, and $\bar{\alpha} = 1$ indicates the same magnitude of birds moving in and out of view.

Species misidentification

Observers recorded the counts of each species i , which required correctly identifying individuals to species. Despite rigorous training and experience, species misidentification can occur during the observation process (Johnston et al., 2015). For a given species i , the observed number of individuals contains the number of correctly identified individuals of species i in addition to false positives (i.e., individuals from species k misidentified by the observer as species i). There may also be individuals of species i misidentified as species k . Again, we considered the true bird species composition, π , and we defined

the bird species composition seen by the observers as ϕ . We can use the conditional probability $(\phi_k | \pi_i)$ to estimate how many individuals of species i were misidentified as species k . These conditional probabilities are contained within a square $i \times k$ matrix, where elements along the diagonal are the probabilities of correctly identifying species i , $(\phi_{k=i} | \pi_i)$, and off-diagonal elements contain the misidentification probabilities $(\phi_{k \neq i} | \pi_i)$. We use Equation (5) to describe this observational process with a multinomial distribution:

$$C_{jik} \sim \text{multinomial}((\phi_k | \pi_i), N_{ji}), \tag{5}$$

where the species-specific available latent abundance, N_{ji} , for each species i in transect j is distributed into the elements C_{jik} , which contain the additional dimension k . We define this latent value, C_{jik} , as the scalar elements of the confusion matrix for each transect j , representing the number of individuals of species i that were correctly identified (diagonal elements, $k = i$) and incorrectly identified (off-diagonal elements, $k \neq i$). Using the $i \times k$ confusion matrix, the sum of column k (i.e., $\sum_i C_{jik}$) is the number of individuals of species k recorded under perfect detection, including both species correctly identified ($k = i$, diagonal element) and misidentified ($k \neq i$,

off-diagonal elements), which might also include individuals counted by the aerial observers that were not captured by the camera. Then, we sum across columns $k = 1, \dots, K$ species (i.e., $\sum_k \sum_i C_{jik}$), which collapses the species-specific abundances to the species-wide latent abundance for each transect j . Here, $\sum_k \sum_i C_{jik}$ is equivalent to $\sum_i N_{ji}$, as misidentification only changes the species-specific magnitudes but not the species-wide value.

Imperfect detection

In addition to misidentification, observers may also undercount or overcount the number of individuals in their field of view due to imperfect detection. We can describe this process using a binomial distribution as in Equation (6); we use i to denote true species identification from the photographs and k to denote observed species identification from real-time observations:

$$\sum_k \text{OBS}_{jko} \sim \text{binomial}\left(\bar{p}_o \sum_i N_{ji}\right), \quad (6)$$

where $\sum_k \text{OBS}_{jko}$ are data containing the observed bird species-wide counts for each observer o and transect j . Detection probability, \bar{p}_o , is the mean observer- and species-specific detection probability; and $\sum_i N_{ji}$ (i.e., $\sum_k \sum_i C_{jik}$) is the species-wide number of individuals. By including movement, imperfect detection, and misidentification, the model can account for both undercounting and overcounting individual birds.

Model identifiability

As noted above, the data and the structure of the model did not allow for separately estimating movement rate and detection probability. However, the mathematical product of these parameters, $\bar{\alpha} \times \bar{p}_o = \bar{\epsilon}_o$, is estimable, giving us the modified species-wide observation process illustrated in Equation (7):

$$\sum_k \text{OBS}_{jko} \sim \text{Poisson}(\Lambda \times \bar{\epsilon}_o). \quad (7)$$

Here, we summed the observer data across species and described the data with a Poisson distribution. The expected value of the distribution is the product of the expected bird species-wide abundance, movement rate, and detection probability. We generalize the combination of movement and detection to estimate $\bar{\epsilon}_{jo}$ specific to each transect and observer, allowing us to account for

potential differences in $\bar{\epsilon}_o$ due to the seat assignment (middle or rear) of observer, o , during transect, j , as described by Equation (8):

$$\log(\bar{\epsilon}_{jo}) = \bar{\epsilon}_o + \beta_1 \times \text{seat}_{jo}, \quad (8)$$

where $\bar{\epsilon}_o$ is the estimate for observer o when in the rear seat, β_1 is the additive effect of being in the middle seat, and seat_{jo} is a binary indicator (1 for middle seat, 0 for rear seat) for each transect j and observer o .

We cannot fully estimate the confusion matrix and associated conditional probabilities owing to differences in the fields of view of the observers compared to the camera and, therefore, the inability to directly compare species identification of birds observed in real time and birds captured by the camera. However, we simply corrected for misidentification by specifying it as a rate, $\phi_{ok=oi}/\pi_i$, the rate at which species i is correctly identified, by observer o ($\phi_{ok=i}/\pi_i = 1$ when no misidentification occurs and $\phi_{ok=i}/\pi_i \neq 1$ when misidentification occurs). Thus, we used Equation (9) to estimate the observed bird species composition, ϕ_{ok} , with a multinomial distribution and observer data:

$$\text{OBS}_{jko} \sim \text{multinomial}\left(\phi_{ok}, \sum_k \text{OBS}_{jko}\right), \quad (9)$$

where ϕ_{ok} is the proportion of species identified by an observer, o , as species, k .

Out-of-sample correction

We can use the estimated parameters (i.e., $\bar{\epsilon}_o, \pi_i, \phi_{ok}$) to correct for out-of-sample observations made when photographic data do not exist (Figure 1). We used Equation (10) to model species-specific observation data with a Poisson distribution:

$$\text{OBS}_{jko} \sim \text{Poisson}(\lambda_i \times \phi_{o,k=i}/\pi_i \times \bar{\epsilon}_o). \quad (10)$$

Therefore, by combining the new observation data with the estimated parameters, we can calculate the parameter of interest, λ_i . The estimated correction factor, CF, for each species and observer is $\widehat{\text{CF}}_{io} = \phi_{o,k=i}/\pi_i \times \bar{\epsilon}_o$.

Parameter estimation

We fit our model using a Markov Chain Monte Carlo (MCMC) approach (Casella & George, 1992; Gelfand & Smith, 1990; Geman & Geman, 1993). We fit the model in the R package NIMBLE version 0.6-10

(de Valpine et al., 2017) in R version 4.0 (R Core Team, 2020) with 3 chains, a burn-in of 10,000 iterations, and a sampling period of 20,000 iterations. We used the R packages coda (Plummer et al., 2006), ggcmc (Fernández-i-Marín, 2016), and MCMCvis (Youngflesh, 2018) to inspect model convergence using trace plots, density plots, and Gelman–Rubin statistic, \hat{R} , values (Gelman & Rubin, 1992). We used vague priors, including the log of $\lambda_i \sim \text{Normal}(0, 100)$, $\phi_{ok} \sim \text{Dirichlet}(1)$, $\bar{\epsilon}_o \sim \text{Normal}(0, 100)$, and $\beta_1 \sim \text{Normal}(0, 100)$.

Model testing

Although the photographs provided a useful approximation of the true number and species composition of birds, using photographs does not capture truth as well as known animal numbers, which can be accomplished using captive animals (Zabel et al., 2023). However, we can use simulations to similarly test our ability to accurately estimate the species-specific number of birds, which has an additional benefit of out-of-sample validation, which is absent when using captive animals. We used simulated data to evaluate the model's ability to correctly return parameter estimates for out-of-sample predictions (see Appendix S1 for full description of model testing methods). For the simulation of observer data, we simplified the model to only include one observer and did not include a seat assignment covariate. We generated a parameter value for the true movement while also generating an offset (between 1 and 1.5) that allowed for a larger field of view for observers compared to the camera. Similarly, we generated probabilities of misidentification (pairwise values across all species) and detection (one value assigned for all species) and the true species composition for each simulated transect. We used the generated misidentification values to construct a species \times species confusion matrix for each transect. Using the generated values for true movement and true composition, we simulated species-specific data for the camera. Data and model code for the simulations and empirical model are provided at <https://doi.org/10.5281/zenodo.11111632>.

RESULTS

Summed across all 321 transects, the camera captured 55,000 photographs containing 9029 individual marine birds, whereas observer 1 recorded 6434 birds, and observer 2 recorded 5021. Thirty-one marine bird species were identified across observers and photographs (Table 1). The total number of individuals per species

captured on the camera across all transects ranged from 2 (Black Scoter, *Melanitta americana*) to 1644 (Bufflehead, *Bucephala albeola*). The camera captured 1612 groups of marine birds across all transects, ranging from 1 to 518 birds per group with a mean of 5.60 birds per group (SD = 19.16). Group size was left skewed: 79% of groups had ≤ 5 birds and 91% had ≤ 10 birds. Including only birds that could be identified to species, 27% of groups captured by the camera included more than one species.

Both observers tended to undercount birds compared to the camera (Figure 2); observer 1 recorded a mean of 78.9% (SD = 1.2%) of the birds caught on the camera per transect, and observer 2 recorded a mean of 68.7% (SD = 1.0%). However, both observers counted more birds than caught on the camera on some transects (28.3% of the transects for observer 1 and 25.2% of the transects for observer 2). The species with the smallest difference in total counts between observer and camera was Barrow's Goldeneye (observer 1 total was 96.7% of the camera total) and Brant (*Branta bernicla*; observer 2 total was 100.4% of the camera total). The species with the greatest difference in counts between observer and camera were Pelagic Cormorant (*Phalacrocorax pelagicus*; observer 1 total was 10.6% of the camera total) and Northern Pintail (*Anas acuta*; observer 2 total was 1.4% of the camera total).

The results from our simulations indicated that our model was able to capture the data-generating parameters accurately. The simulations resulted in a 100% convergence rate for $\bar{\epsilon}$ with minimal bias ($< -0.01\%$, interquartile range [IQR] = -0.05 to 0.04), a 96.2% convergence rate for λ with minimal bias (0.01% , IQR = -0.06 to 0.08), and a 98.2% convergence rate for Λ with minimal bias ($< 0.01\%$, IQR = -0.05 to 0.07).

Based on model diagnostics and general agreement between our corrected counts and our camera counts, our model appeared to perform well on the empirical dataset. Overall diagnostics indicated that our models converged; although, we had \hat{R} estimates > 1.1 for Ancient Murrelet CF and Black Scoter CF (Appendix S2: Table S1), which had very few observations (Table 1). Using the data collected from one camera and two observers over 321 transects, the fine-grained model required < 1 min to compile and build in NIMBLE and 42 min and 33.27 MB of memory to run. Correction factor estimates varied across species/species groups and between observers (Appendix S2: Table S1; Figure 3). For most species/species groups, our calculated corrected counts (calculated by multiplying the inverse of our correction estimates from our model by the observer counts) were very similar to the counts from the camera. As one

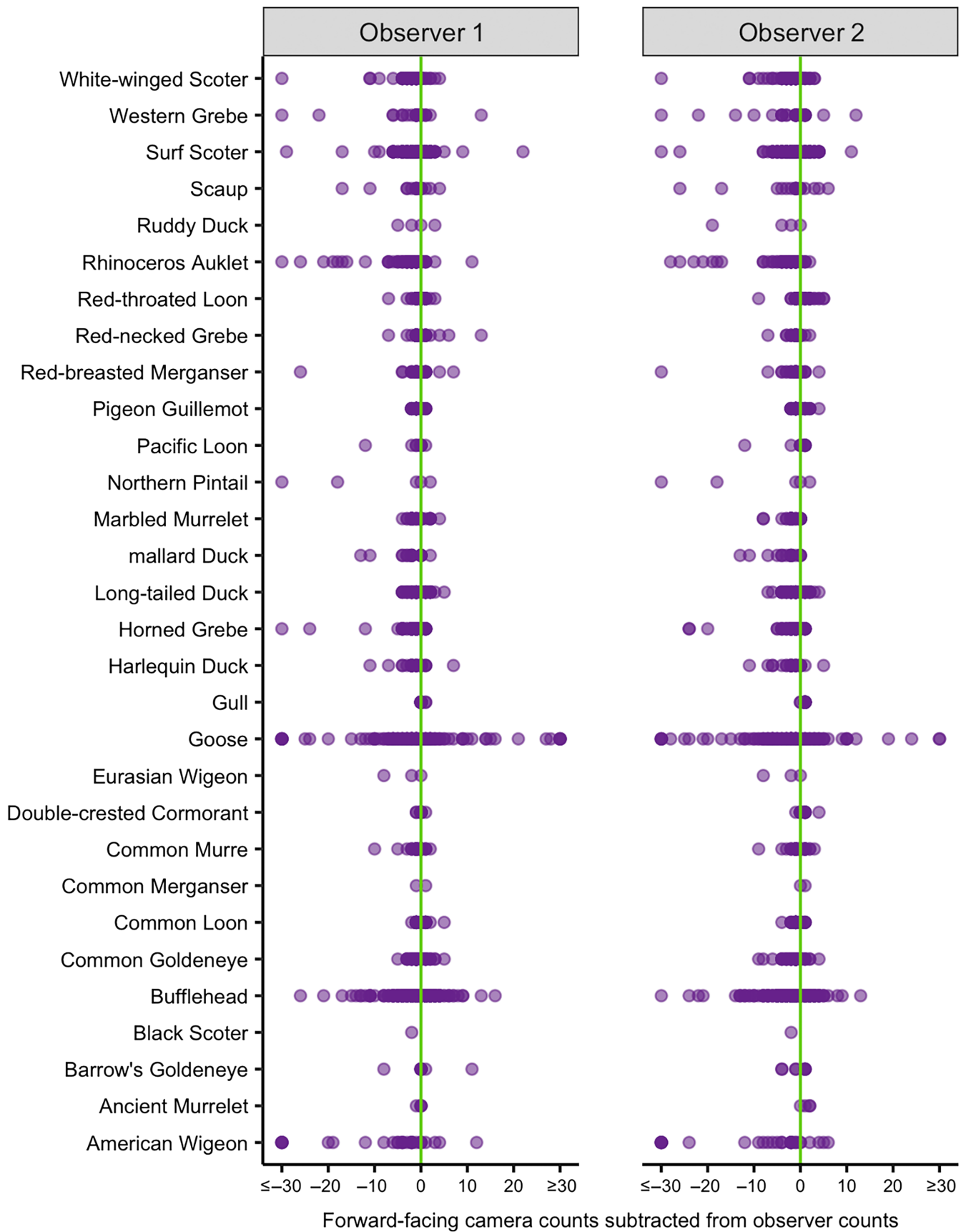


FIGURE 2 Observer count accuracy per species. Points display the count captured by the camera subtracted from each observer's count for each species for each group of birds observed. Only groups that were captured by the camera were included.

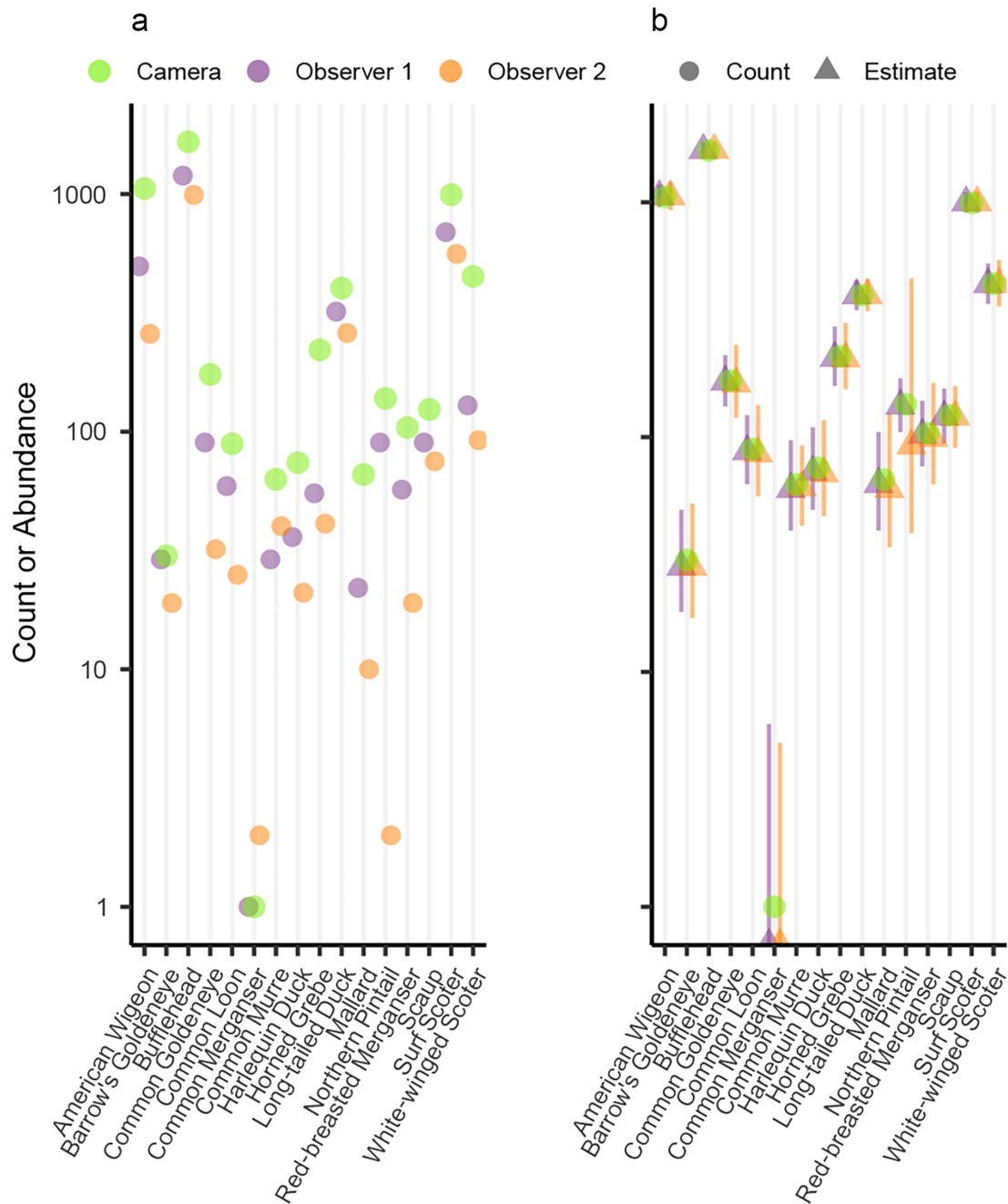


FIGURE 3 Model performance for count corrections: (a) raw counts from the observers or camera (points); (b) counts from the camera (points) and the estimated abundances produced by our model (triangles) for select species. Error bars on estimates indicate 95% credible intervals. The y-axis is on logarithmic scale.

would expect, the model tended to produce correction estimates that yielded corrected counts proportionally closer to the counts of the camera for species with larger sample sizes. The seat position of the observer had a negligible effect on detection/species identification (taxonomically fine-grained analysis: $\beta_1 = -0.001$, 95% credible interval = -0.04 to 0.04 ; taxonomically coarse-grained analysis: $\beta_1 = -0.002$, 95% credible interval = -0.04 to 0.03).

DISCUSSION

Comparing detected animals to known numbers of animals can be an effective method for estimating measurement errors and adjusting abundance estimates to improve the accuracy of wildlife monitoring data (Bayliss & Yeomans, 1990; Caughley et al., 1976; Pearse et al., 2008; Zabel et al., 2023). Our results suggest that uncorrected counts from aerial surveys of marine birds in

the Salish Sea include notable measurement error resulting from some combination of animal movement in response to the plane, imperfect detection, and species misidentification. Comparing real-time observations of bird counts from aerial surveys, especially with multiple species, to counts from photographs taken of the area in front of the plane is a complicated process because animal movement, detection, and species identification cannot be separately estimated. Therefore, it is impossible to determine whether an individual captured by the camera but not by an observer resulted from the bird not being available for detection, the observer not detecting the bird, or the observer detecting the bird but identifying it as the incorrect species. As is common in other studies investigating observation errors from aerial surveys (Alisauskas & Conn, 2019; Caughley et al., 1976; Pearse et al., 2008), observers counted fewer individuals than were in the population of interest (i.e., in the photographs from the camera), and measurement error varied by species and observer. Applying the correction factors that we estimated to the observer counts yielded accurate estimates based on comparison with the camera counts.

At its most basic level, our study demonstrates that the ability to detect and correctly identify marine bird species from aircraft varies both across observers and species, reinforcing that estimates correcting for biases must account for, at minimum, these two factors. Although multiple methods to account for imperfect detection of wildlife in aerial surveys have emerged, many of these approaches either do not mimic the actual field conditions under which monitoring data are collected, do not account for partial availability, or fail to account for species misidentification (Davis et al., 2022). Given the ability of our model to provide accurate correction factors for the species in the dataset, our model results can be used to adjust both future and historical counts of marine birds in the Salish Sea aerial survey by the same observers under the assumption that observer performance is constant over time. For surveys with the same observers, marine bird wintering counts can be retroactively adjusted to improve the ability of the survey to capture true abundance while integrating uncertainty in the observation process into the abundance estimates. However, observers will change over time, as will the abilities of individual observers (Sauer et al., 1994), underscoring the value of repeating the simultaneous collection of observer and photographic data as funding allows, when staff turnover occurs, or when conditions that may influence detection are altered (e.g., change of aircraft platform). As our correction-factor results are specific to each observer, further investigation with many different observers could elucidate the magnitude of observer effect.

Although the method we have developed can provide accurate correction factors for most of the species recorded in the survey, the method has limited value when species are rare or highly sensitive to plane presence. Given that the correction is multiplicative, the models we present cannot provide an estimate for the true number of birds present when the observer count for a species is zero. In the data for the current study, observers did not record any observations of Black Scoter or Eurasian Wigeon (*Mareca penelope*), but the camera captured both. From the surveys alone, one could erroneously but reasonably conclude that neither of these species were present on the transects. Black Scoter was only captured by the camera on one transect, and one observer may have seen the same animal and identified it as an unknown scoter. Eurasian Wigeon were identified in mixed groups with American Wigeon, which substantially outnumber the Eurasian Wigeon. Others have also noted that less numerous species in mixed groups may receive disproportionately lower counts or may not be recognized as separate species (Gilbert et al., 2021). Additional surveys might have provided nonzero detections and additional captures of these rarely sighted species wintering in the Salish Sea, which could produce more accurate abundance estimates.

Although our correction estimates are specific to the Salish Sea, specific characteristics of the survey (e.g., aircraft used and altitude flown), observers, and species recorded during the surveys, our approach has potential to be useful for other monitoring programs, especially those using multiple observers and in study regions where the ability to account for imperfect detection using double observer methods or multiple survey platforms is logistically prohibitive. Researchers can mimic our field approach and apply our model to their own data to estimate their own correction factors. Several expansions and refinements are also possible. Future applications may benefit from using an array of point-of-view cameras that accurately capture the same field of view as the observers. This source of data would allow for the development of a detection model that accounts for group size. As demonstrated in other studies investigating detection probabilities in aerial surveys (Clement et al., 2017; Cook & Jacobson, 1979; Gilbert et al., 2021; Pearse et al., 2008), group size can affect the detection probabilities of observers. However, achieving an exactly equivalent field of view between observers and cameras could be difficult in practice because observers would need to maintain fixed head and eye positions throughout each transect. Future applications of our general approach could also implement artificial intelligence-based software for wildlife counts from photographs to reduce image processing time;

however, this approach might not work well for mixed-species flocks (Marchowski, 2021).

Advances in plane-based or autonomous aerial vehicle-based photography, coupled with artificial intelligence-based analysis of images, have the potential to transform aerial monitoring of wildlife (e.g., Chabot et al., 2018; Marchowski, 2021; Qian et al., 2023). Removing the reliance on plane-based observers with photographic images that can be saved and revisited over time as technology improves could address many of the challenges of observer-based surveys. However, to be viable, surveys of this type will have to be of sufficiently high quality and low cost, and the timeline for development of the technology necessary to facilitate such surveys is uncertain. In multispecies systems, this timeline is likely to be extended. Further, using autonomous aerial vehicle-based photography for aquatic birds can come with additional challenges of disturbing flying birds (e.g., birds potentially fleeing the area or attacking the vehicles) and requiring personnel highly trained in both target species biology and autonomous aerial vehicle operation (Marchowski, 2021).

Many wildlife population and community analyses require accurate long-term monitoring of abundance to inform species management or address scientific hypotheses (Nichols & Williams, 2006; Tinkle, 1979). Inaccurate abundance estimates can lead to poor management decisions or erroneous scientific conclusions (Elliot et al., 2020; Ward-Paige et al., 2010). By means of a small supplemental study using cameras to compare observed counts to known counts from photographs, we have shown that it is possible to account for multiple sources of measurement error, including animal movement, imperfect detection, and species misidentification. Additionally, we have demonstrated how to apply estimated correction factors retroactively to existing data. Our results contribute to a growing recognition of the need for tools to improve abundance estimates from aerial-based survey counts. The ability to maintain long-term aerial monitoring efforts while simultaneously improving our confidence in the estimates and trends obtained from them is imperative for the management of wildlife populations.

AUTHOR CONTRIBUTIONS

Conceptualization: Kyle A. Spragens, Joseph Evenson, and Emily Silverman. *Data curation:* Jamie L. Brusa. *Data collection:* Joseph Evenson, Bryan Murphie, Thomas A. Cyra, and Heather J. Tschaekofske. *Formal analysis:* Jamie L. Brusa, Matthew T. Farr, and Sarah J. Converse. *Funding acquisition:* Sarah J. Converse, Kyle A. Spragens, and Joseph Evenson. *Investigation:* Jamie L. Brusa, Matthew T. Farr, Kyle A. Spragens, Joseph Evenson, Emily Silverman, Sarah J. Converse, and Heather J. Tschaekofske. *Methodology:* Jamie L. Brusa, Matthew

T. Farr, Kyle A. Spragens, Joseph Evenson, Emily Silverman, Sarah J. Converse, Bryan Murphie, and Thomas A. Cyra. *Project administration:* Kyle A. Spragens and Sarah J. Converse. *Visualization:* Jamie L. Brusa, Matthew T. Farr, Kyle A. Spragens, Joseph Evenson, Emily Silverman, and Sarah J. Converse. *Writing—original draft:* Jamie L. Brusa. *Writing—review and edition:* all authors.

ACKNOWLEDGMENTS

Support for Jamie L. Brusa was provided by the US Fish and Wildlife Service via a grant from the Sea Duck Joint Venture. Support for Matthew T. Farr was provided by the Washington Department of Fish and Wildlife. We thank the Washington Cooperative Fish and Wildlife Research Unit for facilitating funding. Chuck Perry with Kenmore Air served as the pilot on all flights. Any use of trade, firm, or product names is for descriptive purposes only and does not imply endorsement by the US Government.

CONFLICT OF INTEREST STATEMENT

The authors declare no conflicts of interest.

DATA AVAILABILITY STATEMENT

Code and data (Brusa et al., 2024) are available from Zenodo: <https://doi.org/10.5281/zenodo.11111632>.

ORCID

Jamie L. Brusa  <https://orcid.org/0000-0003-4787-0460>

Matthew T. Farr  <https://orcid.org/0000-0003-1011-6851>

REFERENCES

- Alisauskas, R. T., and P. B. Conn. 2019. "Effects of Distance on Detectability of Arctic Waterfowl Using Double-Observer Sampling during Helicopter Surveys." *Ecology and Evolution* 9: 859–867.
- Anderson, E. M., J. L. Bower, D. R. Nysewander, J. R. Evenson, and J. R. Lovvorn. 2009. "Changes in Avifaunal Abundance in a Heavily Used Wintering and Migration Site in Puget Sound, Washington, during 1966–2007." *Marine Ornithology* 37: 19–27.
- Bayliss, P., and K. M. Yeomans. 1990. "Use of Low-Level Aerial Photography to Correct Bias in Aerial Survey Estimates of Magpie Goose and Whistling Duck Density in the Northern Territory." *Australian Wildlife Research* 17: 1–10.
- Béchet, A., A. Reed, N. Plante, J.-F. Giroux, and G. Gauthier. 2004. "Estimating the Size of the Greater Snow Goose Population." *The Journal of Wildlife Management* 68: 639–649.
- Bishop, E., G. Rosling, P. Kind, and F. Wood. 2016. "Pigeon Guillemots on Whidbey Island, Washington: A Six-Year Monitoring Study." *Northwestern Naturalist* 97: 237–245.
- Blight, L. K., K. A. Hobson, T. K. Kyser, and P. Arcese. 2015. "Changing Gull Diet in a Changing World: A 150-Year Stable Isotope ($\delta^{13}\text{C}$, $\delta^{15}\text{N}$) Record from Feathers Collected in the

- Pacific Northwest of North America.” *Global Change Biology* 21: 1497–1507.
- Bower, J. L. 2009. “Changes in Marine Bird Abundance in the Salish Sea: 1975 to 2007.” *Marine Ornithology* 37: 9–17.
- Brack, I. V., A. Kindel, and L. F. B. Oliveira. 2018. “Detection Errors in Wildlife Abundance Estimates from Unmanned Aerial Systems (UAS) Surveys: Synthesis, Solutions, and Challenges.” *Methods in Ecology and Evolution* 9: 1864–73.
- Briggs, K. T., W. B. Tyler, and D. B. Lewis. 1985a. “Aerial Surveys for Seabirds: Methodological Experiments.” *The Journal of Wildlife Management* 49: 412–17.
- Briggs, K. T., W. B. Tyler, and D. B. Lewis. 1985b. “Comparison of Ship and Aerial Surveys of Birds at Sea.” *The Journal of Wildlife Management* 49: 405–411.
- Brusa, J. L., M. Farr, and S. Converse. 2024. “Quantitative-Conservation-Lab/Brusa_et_al: Release Version 1.” Zenodo. <https://doi.org/10.5281/zenodo.11111632>.
- Buckland, S. T., D. R. Anderson, K. P. Burnham, J. L. Laake, D. L. Borchers, and L. Thomas. 2001. *Introduction to Distance Sampling: Estimating Abundance of Biological Populations*. Oxford: Oxford University Press.
- Buckley, P. A., and F. G. Buckley. 2000. “The Role of Helicopters in Seabird Censusing.” *Proceedings of the Society of Caribbean Ornithology, Special Publication* 1: 134–147.
- Casella, G., and E. I. George. 1992. “Explaining the Gibbs Sampler.” *The American Statistician* 46: 167–174.
- Caughley, G. 1974. “Bias in Aerial Survey.” *The Journal of Wildlife Management* 38: 921–933.
- Caughley, G., R. Sinclair, and D. Scott-Kemmis. 1976. “Experiments in Aerial Survey.” *The Journal of Wildlife Management* 40: 290–300.
- Chabot, D., C. Dillon, and C. Francis. 2018. “An Approach for Using Off-the-Shelf Object-Based Image Analysis Software to Detect and Count Birds in Large Volumes of Aerial Imagery.” *Avian Conservation and Ecology* 13: 227–251.
- Clement, M. J., S. J. Converse, and J. A. Royle. 2017. “Accounting for Imperfect Detection of Groups and Individuals When Estimating Abundance.” *Ecology and Evolution* 7: 7304–10.
- Conn, P. B., J. L. Laake, and D. S. Johnson. 2012. “A Hierarchical Modeling Framework for Multiple Observer Transect Surveys.” *PLoS One* 7: e42294.
- Cook, R. D., and J. O. Jacobson. 1979. “A Design for Estimating Visibility Bias in Aerial Surveys.” *Biometrics* 35: 735–742.
- Crewe, T., K. Barry, P. Davidson, and D. Lepage. 2012. “Coastal Waterbird Population Trends in the Strait of Georgia 1999–2011: Results from the First 12 Years of the British Columbia Coastal Waterbird Survey.” *British Columbia Birds* 22: 8–35.
- Davis, K. L., E. D. Silverman, A. L. Sussman, R. R. Wilson, and E. F. Zipkin. 2022. “Errors in Aerial Survey Count Data: Identifying Pitfalls and Solutions.” *Ecology and Evolution* 12: e8733.
- de Valpine, P., D. Turek, C. J. Paciorek, C. Anderson-Bergman, D. T. Lang, and R. Bodik. 2017. “Programming with Models: Writing Statistical Algorithms for General Model Structures with NIMBLE.” *Journal of Computational and Graphical Statistics* 26: 403–413.
- Elliot, N. B., A. Bett, M. Chege, K. Sankan, N. de Souza, L. Kariuki, F. Broekhuis, P. Omondi, S. Ngene, and A. M. Gopalaswamy. 2020. “The Importance of Reliable Monitoring Methods for the Management of Small, Isolated Populations.” *Conservation Science and Practice* 2: e217.
- Evenson, J. R., H. Tschaekofske, B. Murphie, T. Cyra, and D. Kraege. 2013. *Status and Summary of the 2013 WDFW Winter Sea Duck Aerial Survey Detectability Project – Phase 3*. Olympia, WA: Washington Department of Fish and Wildlife. 35 pp.
- Fernández-i-Marín, X. 2016. “ggmcmc: Analysis of MCMC Samples and Bayesian Inference.” *Journal of Statistical Software* 70: 1–20.
- Frederick, P. C., B. Hylton, J. A. Heath, and M. Ruane. 2003. “Accuracy and Variation in Estimates of Large Numbers of Birds by Individual Observers Using an Aerial Survey Simulator.” *Journal of Field Ornithology* 74: 281–87.
- Gaydos, J. K., and S. F. Pearson. 2011. “Birds and Mammals that Depend on the Salish Sea: A Compilation.” *Northwestern Naturalist* 92: 79–94.
- Gelfand, A. E., and A. F. M. Smith. 1990. “Sampling-Based Approaches to Calculating Marginal Densities.” *Journal of the American Statistical Association* 85: 398–409.
- Gelman, A., and D. B. Rubin. 1992. “Inference from Iterative Simulation Using Multiple Sequences.” *Statistical Science* 7: 457–472.
- Geman, S., and D. Geman. 1993. “Stochastic Relaxation, Gibbs Distributions and the Bayesian Restoration of Images.” *Journal of Applied Statistics* 20: 25–62.
- Gilbert, A. D., C. N. Jacques, J. D. Lancaster, A. P. Yetter, and H. M. Hagy. 2021. “Visibility Bias of Waterbirds during Aerial Surveys in the Nonbreeding Season.” *Wildlife Society Bulletin* 45: 6–15.
- Johnston, A., C. B. Thaxter, G. E. Austin, A. S. C. P. Cook, E. M. Humphreys, D. A. Still, A. Mackay, R. Irvine, A. Webb, and N. H. K. Burton. 2015. “Modelling the Abundance and Distribution of Marine Birds Accounting for Uncertain Species Identification.” *Journal of Applied Ecology* 52: 150–160.
- Lamprey, R., F. Pope, S. Ngene, M. Norton-Griffiths, H. Frederick, B. Okita-Ouma, and I. Douglas-Hamilton. 2020. “Comparing an Automated High-Definition Oblique Camera System to Rear-Seat-Observers in a Wildlife Survey in Tsavo, Kenya: Taking Multi-Species Aerial Counts to the Next Level.” *Biological Conservation* 241: 108243.
- MacKenzie, D. I., J. D. Nichols, G. B. Lachman, S. Droege, J. Andrew Royle, and C. A. Langtimm. 2002. “Estimating Site Occupancy Rates When Detection Probabilities Are Less than One.” *Ecology* 83: 2248–55.
- Marchowski, D. 2021. “Drones, Automatic Counting Tools, and Artificial Neural Networks in Wildlife Population Censusing.” *Ecology and Evolution* 11: 16214–27.
- Miller, A., J. E. Elliott, K. H. Elliott, M. F. Guigueno, L. K. Wilson, S. Lee, and A. Idrissi. 2015. “Brominated Flame Retardant Trends in Aquatic Birds from the Salish Sea Region of the West Coast of North America, Including a Mini-Review of Recent Trends in Marine and Estuarine Birds.” *Science of the Total Environment* 502: 60–69.
- Miller, D. A., J. D. Nichols, B. T. McClintock, E. H. C. Grant, L. L. Bailey, and L. A. Weir. 2011. “Improving Occupancy Estimation When Two Types of Observational Error Occur: Non-Detection and Species Misidentification.” *Ecology* 92: 1422–28.

- Nichols, J. D., and B. K. Williams. 2006. "Monitoring for Conservation." *Trends in Ecology & Evolution* 21: 668–673.
- Pearse, A. T., P. D. Gerard, S. J. Dinsmore, R. M. Kaminski, and K. J. Reinecke. 2008. "Estimation and Correction of Visibility Bias in Aerial Surveys of Wintering Ducks." *The Journal of Wildlife Management* 72: 808–813.
- Pearson, S. F., and N. J. Hamel. 2013. *Marine and Terrestrial Bird Indicators for Puget Sound*. Olympia, WA: Washington Department of Fish and Wildlife and Puget Sound Partnership. 55 pp.
- Plummer, M., N. Best, K. Cowles, and K. Vines. 2006. "CODA: Convergence Diagnosis and Output Analysis for MCMC." *R News* 6: 7–11.
- Pollock, K. H., and W. L. Kendall. 1987. "Visibility Bias in Aerial Surveys: A Review of Estimation Procedures." *The Journal of Wildlife Management* 51: 502–510.
- Qian, Y., G. R. W. Humphries, P. N. Trathan, A. Lowther, and C. R. Donovan. 2023. "Counting Animals in Aerial Images with a Density Map Estimation Model." *Ecology and Evolution* 13: e9903.
- R Core Team. 2020. *R: A Language and Environment for Statistical Computing*. Vienna: R Foundation for Statistical Computing. <https://www.R-project.org/>.
- Royle, J. A., and J. D. Nichols. 2003. "Estimating Abundance from Repeated Presence–Absence Data or Point Counts." *Ecology* 84: 777–790.
- Russell, J., S. Couturier, L. G. Sopuck, and K. Ovaska. 1996. "Post-Calving Photo-Census of the Rivière George Caribou Herd in July 1993." *Rangifer* 16: 319–330.
- Samuel, M. D., and K. H. Pollock. 1981. "Correction of Visibility Bias in Aerial Surveys where Animals Occur in Groups." *The Journal of Wildlife Management* 45: 993–97.
- Sauer, J. R., B. G. Peterjohn, and W. A. Link. 1994. "Observer Differences in the North American Breeding Bird Survey." *The Auk* 111: 50–62.
- Siniff, D. B., and R. O. Skoog. 1964. "Aerial Censusing of Caribou Using Stratified Random Sampling." *The Journal of Wildlife Management* 28: 391–401.
- Strobel, B. N., and M. J. Butler. 2014. "Monitoring Whooping Crane Abundance Using Aerial Surveys: Influences on Detectability." *Wildlife Society Bulletin* 38: 188–195.
- Tinkle, D. W. 1979. "Long-Term Field Studies." *BioScience* 29: 717.
- Vilchis, L. I., C. K. Johnson, J. R. Evenson, S. F. Pearson, K. L. Barry, P. Davidson, M. G. Raphael, and J. K. Gaydos. 2014. "Assessing Ecological Correlates of Marine Bird Declines to Inform Marine Conservation." *Conservation Biology* 29: 154–163.
- Wang, D., Q. Shao, and H. Yue. 2019. "Surveying Wild Animals from Satellites, Manned Aircraft and Unmanned Aerial Systems (UASs): A Review." *Remote Sensing* 11: 1308.
- Ward-Paige, C., J. M. Flemming, and H. K. Lotze. 2010. "Overestimating Fish Counts by Non-Instantaneous Visual Censuses: Consequences for Population and Community Descriptions." *PLoS One* 5: e11722.
- Watson, R. M. 1969. "Aerial Photographic Methods in Censuses of Animals." *East African Agricultural and Forestry Journal* 34: 31–37.
- Weiser, E. L., P. L. Flint, D. K. Marks, B. S. Shults, H. M. Wilson, S. J. Thompson, and J. B. Fischer. 2022. "Optimizing Surveys of Fall-Staging Geese Using Aerial Imagery and Automated Counting." *Wildlife Society Bulletin* 47: e1407.
- Youngflesh, C. 2018. "MCMCvis: Tools to Visualize, Manipulate, and Summarize MCMC Output." *The Journal of Open Source Software* 3: 640.
- Zabel, F., M. A. Findlay, and P. J. C. White. 2023. "Assessment of the Accuracy of Counting Large Ungulate Species (Red Deer *Cervus elaphus*) with UAV-Mounted Thermal Infrared Cameras during Night Flights." *Wildlife Biology* 2023: e01071.

SUPPORTING INFORMATION

Additional supporting information can be found online in the Supporting Information section at the end of this article.

How to cite this article: Brusa, Jamie L., Matthew T. Farr, Joseph Evenson, Emily Silverman, Bryan Murphie, Thomas A. Cyra, Heather J. Tschaekofske, Kyle A. Spragens, and Sarah J. Converse. 2024. "Correcting for Measurement Errors in a Long-Term Aerial Survey with Auxiliary Photographic Data." *Ecosphere* 15(8): e4961. <https://doi.org/10.1002/ecs2.4961>